Stanford Exploration Project, Report 112, November 11, 2002, pages 1–15

Ray based tomography using residual Stolt migration

Robert G. Clapp[1]

ABSTRACT

In complex areas, residual vertical movement is not an effective method to calculate traveltime errors for image domain tomography. By scanning over velocity ratios using residual Stolt migration, a different criteria for a coherent image can be defined, and a traveltime error approximated. The resulting traveltime errors are more accurate, therefore the tomography procedure is more robust than the more traditional methodology. Results are shown on a complex 2-D dataset.

INTRODUCTION

Depth migration is often necessary for complex structures, but requires an accurate interval velocity model. Estimating this velocity model is one of the essential problems in reflection seismology. One of the most common methods to estimate an interval velocity model is from ray-based reflection tomography after migration (Stork, 1992), which I will refer to as image domain tomography. In previous work (Clapp and Biondi, 2000; Clapp, 2001), I showed how to use angle gathers (Prucha et al., 1999; Sava and Fomel, 2000) in conjunction with downward continuation based migration (Gazdag and Sguazzero, 1984; Biondi and Palacharla, 1995) for back-projection. Post-migration reflection tomography is based on the fact that an offset gather (Kirchhoff) or angle gather (wavefield continuation) should be flat after migration. Deviation from flatness indicates a velocity error and can be converted into a travel time error and back-projected. Etgen (1990), among many others, pointed out that, in complex environments, looking at vertical moveout in gathers is not the optimal method to describe moveout errors. Biondi and Symes (2002) presented one alternative approach, constructing gathers where moveout is normal to an event.

Another approach is to use residual migration (Rocca and Salvador, 1982; Levin et al., 1983; Fomel, 1997) to find the best focusing velocity. Stolt (1996) and Sava (1999b,a) showed how to do residual migration for wave continuation methods. These methods allow scanning over slowness field ratios. Audebert et al. (1996) noticed that when scaling the slowness field by a constant, ray behavior is unchanged. Audebert et al. (1997) described a method of updating the velocity model by back projecting along the normal ray.

In this paper I take these works a step further. After performing downward continuation based migration, I use residual migration to find a smooth field of γ values that best focuses

[1]**email:** bob@sep.stanford.edu

the data. I then convert these γ values to approximate travel-time errors and back-project.

I begin by outlining a method of selecting my γ field. I then describe the approximations used to convert γ to $\Delta\mathbf{t}$. Finally, I show the procedure applied to a 2-D North Sea example.

BACKGROUND

Following the methodology of Clapp and Biondi (1999), I will begin by considering a regularized tomography problem. I will linearize around an initial slowness estimate and find a linear operator in the vertical traveltime domain $\mathbf{T}$ that relates change in slowness $\Delta\mathbf{s}$ with our change in traveltimes $\Delta\mathbf{t}$. We will write a set of fitting goals,

$$\begin{aligned} \Delta\mathbf{t} &\approx \mathbf{T}\Delta\mathbf{s} \\ \mathbf{0} &\approx \epsilon\mathbf{A}\Delta\mathbf{s}, \end{aligned} \tag{1}$$

where $\mathbf{A}$ is our steering filter operator (Clapp et al., 1997) and ϵ is a Lagrange multiplier. However, these fitting goals don't accurately describe what we really want. Our steering filters are based on our desired slowness rather than change of slowness. With this fact in mind, we can rewrite our second fitting goal as:

$$\mathbf{0} \approx \epsilon\mathbf{A}(\mathbf{s_0}+\Delta\mathbf{s}) \tag{2}$$

$$-\epsilon\mathbf{A}\mathbf{s_0} \approx \epsilon\mathbf{A}\Delta\mathbf{s}. \tag{3}$$

Our second fitting goal can not be strictly defined as regularization but we can still do a preconditioning substitution (Fomel et al., 1997), giving us a new set of fitting goals:

$$\begin{aligned} \Delta\mathbf{t} &\approx \mathbf{T}\mathbf{A}^{-1}\mathbf{p} \\ -\epsilon\mathbf{A}\mathbf{s_0} &\approx \epsilon\mathbf{I}\mathbf{p}. \end{aligned} \tag{4}$$

The trouble is how to estimate $\Delta\mathbf{t}$. Previously I have calculated semblance at various hyperbolic moveouts. I then picked the moveout corresponding to the maximum semblance. To calculate Δt I converted my picked moveout parameter back to a depth error Δz, which is converted into a travel time. Following the methodology of Stork (1992),

$$\Delta t = \cos(\alpha)\cos(\beta)v\Delta z, \tag{5}$$

where, α is the local dip, β is the opening angle at the reflection point, and v is the local velocity. This approach is effective in areas which are generally flat and have a sufficient offset coverage, but as shown in Biondi and Symes (2002) it runs into problems when these conditions aren't met.

A real data example of this problem can be seen in Figure 1. Note the "hockey stick" behavior seen at 'A'. If we follow the procedure of Stork (1992) we get unreasonably large travel time errors. Clapp (2002) shows that if we use these points for back projection, we get too large of velocity changes, which can lead to instability of the tomography problem.

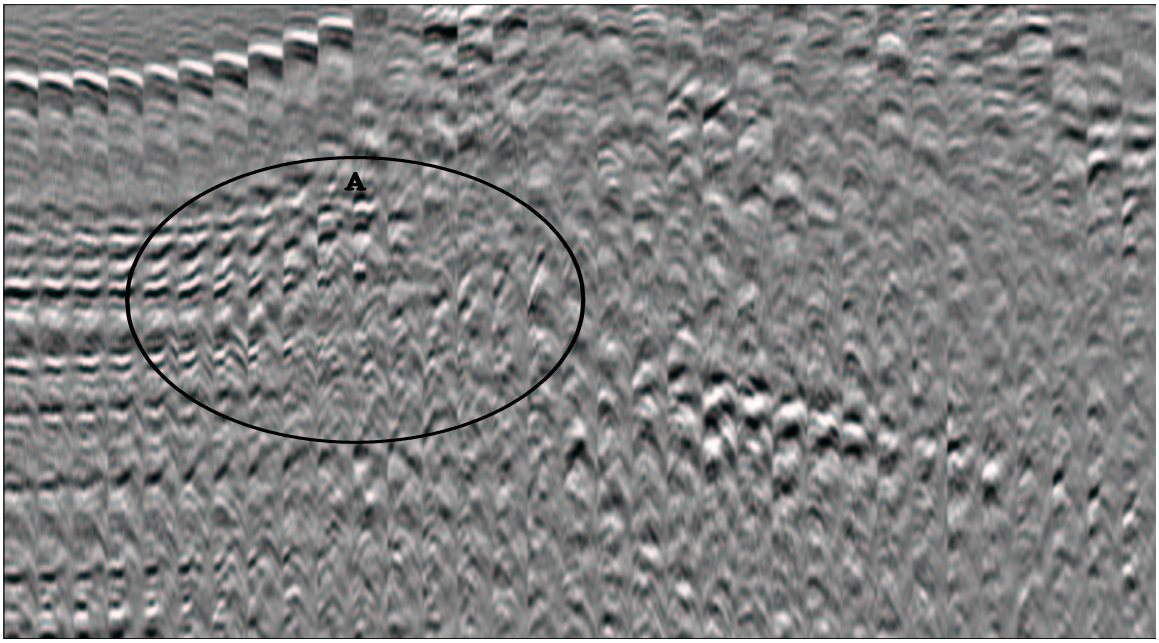

Figure 1: Every 5th gather to the left edge of a salt body. Note the coherent, "hockey stick" behavior within 'A'. bob1-gathers [CR]

METHODOLOGY

Creating a travel time error from residual migration involves several steps. My method is to first perform residual Stolt migration (Stolt, 1996; Sava, 1999b) on offset domain image gathers with a slight twist: minimize reflector movement among the various velocity ratios. I convert the different images to the angle domain (Sava and Fomel, 2000) and calculate the coherence of the zero moveout. I then set up a simple inversion problem to obtain a smooth estimate of γ for each model location. Finally, I convert this γ to an approximate traveltime error and back project it.

Residual Stolt migration

The main idea of Sava (1999b) is that we can do residual Stolt migration by defining the updated depth wave number k_z for various velocity ratios γ through the equation

$$k_z = \frac{1}{2}\sqrt{\frac{1}{\gamma^2}\frac{\left[4k_{z_0}^2+\left(\left|\vec{k}_m+\vec{k}_h\right|-\left|\vec{k}_m-\vec{k}_h\right|\right)^2\right]\left[4k_{z_0}^2+\left(\left|\vec{k}_m+\vec{k}_h\right|+\left|\vec{k}_m-\vec{k}_h\right|\right)^2\right]}{16k_{z_0}^2}-\left|\vec{k}_m-\vec{k}_h\right|^2} + \frac{1}{2}\sqrt{\frac{1}{\gamma^2}\frac{\left[4k_{z_0}^2+\left(\left|\vec{k}_m+\vec{k}_h\right|-\left|\vec{k}_m-\vec{k}_h\right|\right)^2\right]\left[4k_{z_0}^2+\left(\left|\vec{k}_m+\vec{k}_h\right|+\left|\vec{k}_m-\vec{k}_h\right|\right)^2\right]}{16k_{z_0}^2}-\left|\vec{k}_m+\vec{k}_h\right|^2}, \tag{6}$$

where

- k_{z0} and k_z are depth wavenumbers before and after residual migration,
- $\mathbf{v_0}$ the background velocity field,
- γ is defined as the $\frac{\mathbf{v_0}}{\mathbf{v_n}}$, and
- $\vec{k}_m$ and $\vec{k}_h$ are the offset and midpoint wavenumbers.

To make sure that residual Stolt migration behaves as we anticipate, I perform a test on the Marmousi synthetic. The top panel of Figure 2 shows every 15th common reflection point (CRP) gather of the Marmousi synthetic migrated with the correct velocity. Note how the CRP gathers are generally flat. The middle panel shows the same CRP gathers after migrating the data with a velocity 3% lower. The focusing has degraded and moveout in the gathers has increased. The bottom panel shows the result of performing residual migration with a γ value of .97. Note how, as expected, the image is better focused and the gathers are flatter.

Figure 3 shows an angle image gather for seven different values of γ ranging from .8 to 2.0. Note how we see the events move from curving down (left) to curving (up) as we increase γ. Unfortunately, the events also move as we change γ. We can eliminate this movement for flat events, and reduce it significantly for dipping events, by modifying our equation for k_z,

$$\begin{aligned} k_z = &\frac{1}{2}\sqrt{\frac{\left[4k_{z_0}^2+\left(\left|\vec{k}_m+\vec{k}_h\right|-\left|\vec{k}_m-\vec{k}_h\right|\right)^2\right]\left[4k_{z_0}^2+\left(\left|\vec{k}_m+\vec{k}_h\right|+\left|\vec{k}_m-\vec{k}_h\right|\right)^2\right]}{16k_{z_0}^2}-\gamma^2\left|\vec{k}_m-\vec{k}_h\right|^2} \\ &+\frac{1}{2}\sqrt{\frac{\left[4k_{z_0}^2+\left(\left|\vec{k}_m+\vec{k}_h\right|-\left|\vec{k}_m-\vec{k}_h\right|\right)^2\right]\left[4k_{z_0}^2+\left(\left|\vec{k}_m+\vec{k}_h\right|+\left|\vec{k}_m-\vec{k}_h\right|\right)^2\right]}{16k_{z_0}^2}-\gamma^2\left|\vec{k}_m+\vec{k}_h\right|^2}. \end{aligned} \tag{7}$$

Figure 4 shows the same image gather using equation (7). The reflector movement is generally eliminated from the gather.

Gamma selection

After performing the residual Stolt migration and converting to the angle domain, I am left with a volume of dimension $v(z,\alpha,x,\gamma)$, where α is aperture angle. From this volume we need to pick the best γ as a function of x and z. I also have the problem that even with the redefinition of the residual Stolt migration problem in Equation (7), events still have some movement at different γ's. For now I will ignore the movement problem on the theory that as long as we tend towards the correct solution, the best focusing γ will tend towards 1 and the amount of mispositioning at the best focusing γ will decrease.

For now I took a rather simple approach. I calculated the semblance for flat events at the different γ values. I then picked the best γ ratio at each location. I used this field as my data **d**. I used the maximum semblance at each location as a weighting operator **W** to give more preference to strong events. I used a 2-D gradient operator for my regularization operator **A** and solved the inversion problem defined by the fitting goals,

$$\begin{aligned} \mathbf{0} &\approx \mathbf{W}(\mathbf{d}-\mathbf{m}) \\ \mathbf{0} &\approx \epsilon\mathbf{A}\mathbf{m}, \end{aligned} \tag{8}$$

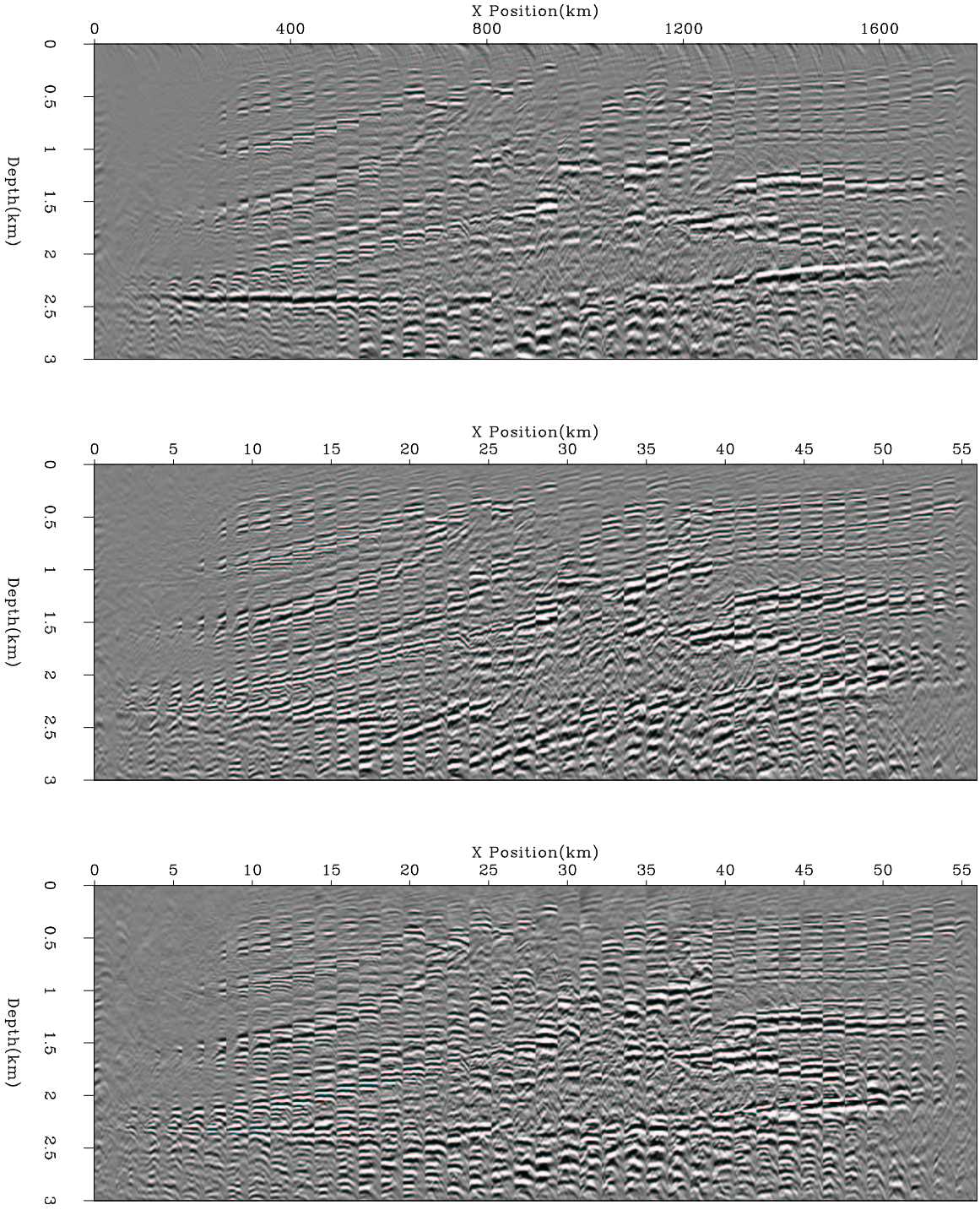

Figure 2: The top panel is the Marmousi synthetic migrated with the correct velocity. The center panel is the result of migrating with a velocity 3% less. The bottom panel is the result of residual Stolt migration with $\gamma = 97\%$. Note how the gathers are almost as flat as in the original migration. bob1-marm1 [CR,M]

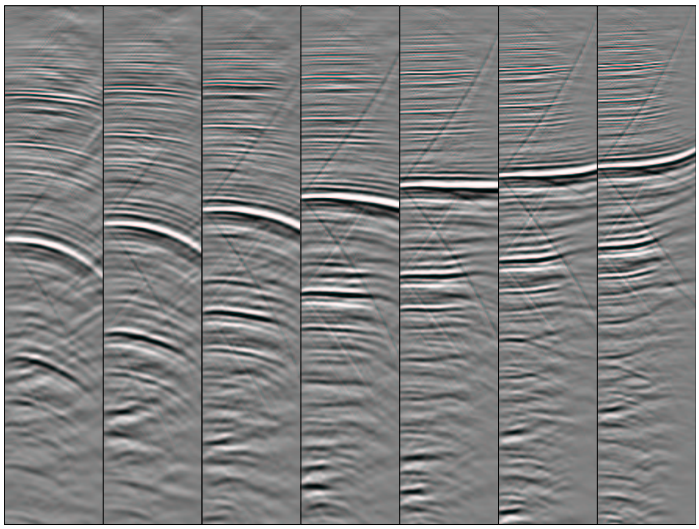

Figure 3: CRP gathers after performing residual Stolt migration with a γ value between .80 and 1.20. Note the significant reflector movement. bob1-moveme [CR,M]

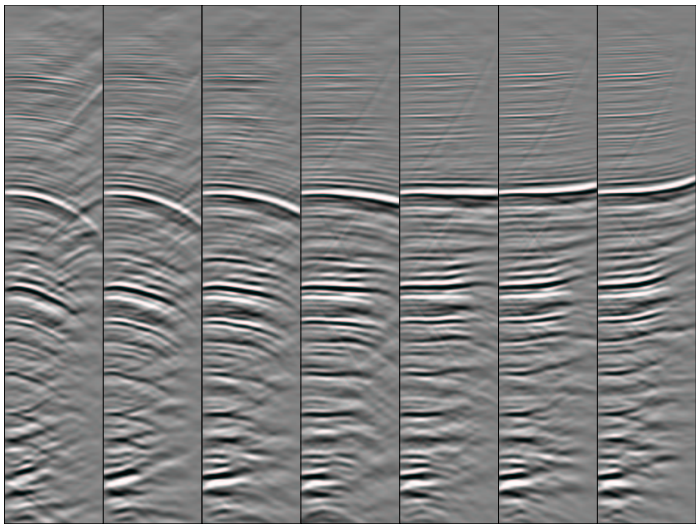

Figure 4: CRP gathers after performing residual Stolt migration using Equation 7. Note the lack of movement compared to Figure 3. bob1-nomove [CR,M]

where ϵ is the amount of relative smoothing and **m** is the resulting model. A better method, and a topic for future work, would be to calculate the semblance for a range of moveouts and do a non-linear search for a smooth γ function.

To test whether the method works I scanned over γ values from .95 to 1.05 on the migration result shown in the center panel of Figure 2. The left panel of Figure 5 shows the selected ratio, **m**, in fitting goals (8) and the right panel shows a histogram of the picked values. Note how we have generally picked the correct γ value ($\gamma = .97$).

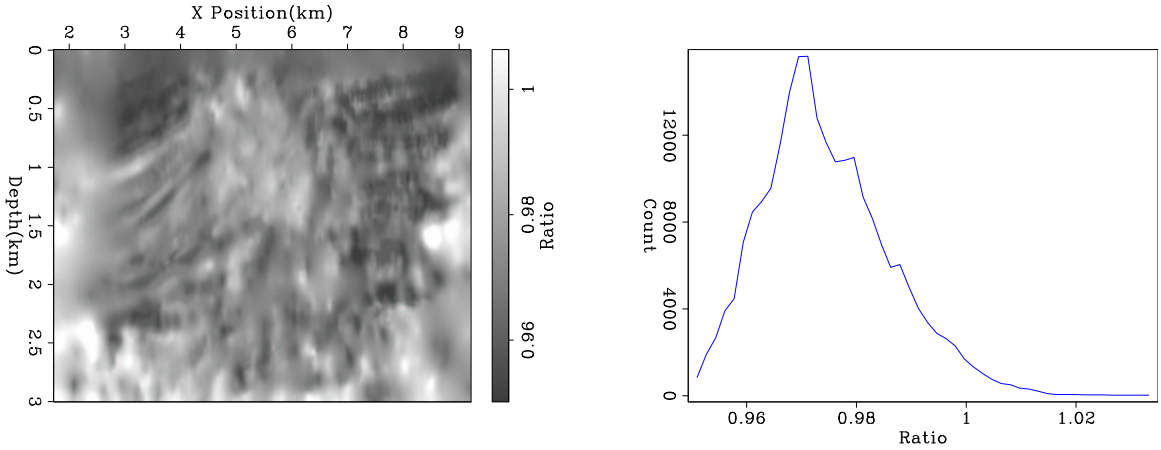

Figure 5: The left plot is the selected γ value using fitting goals (8). The right panel is a histogram of the picked values. Note the peak at approximately .97, the inverse of the velocity scaling. bob1-pick [CR,M]

Back projection

Converting the γ value into the $\Delta\mathbf{t}$ term needed for tomography is troublesome. Etgen (1990) showed that residual migration R_{mig} is the vector sum of residual normal moveout R_{nmo}, residual dip moveout R_{dmo} and residual zero offset migration R_{zoff} components. What we want to back project in image domain tomography is the R_{nmo} and R_{dmo} components. We can use simple trigonometry to convert a γ term to an approximate R_{nmo} term through

$$\Delta t(\mathbf{x},\alpha) = (\gamma - 1) * \left(\frac{1}{\cos(\alpha)} - 1 \right), \tag{9}$$

where $t(\mathbf{x},\alpha)$ is the traveltime to the surface of ray pair starting from **x** at the opening angle α. This approximation is not accurate, but has approximately the correct behavior.

EXAMPLE

To test the methodology I chose a 2-D line from a 3-D North Sea dataset. Figure 6 shows

- the initial velocity model (top-left panel),
- the initial migration (top-right), and
- a zoomed in portion of the model with three regions highlighted for future comparisons (bottom).

I performed one non-linear iteration of tomography using three different approaches. The top panel of Figure 7 shows the result of using vertical moveout as the basis for determining the time errors. The center panel is again the result of using vertical moveout for the time error calculation with additional constraints on what points are used for back projection and limiting the effect of bad moveouts (Clapp, 2002). The bottom panel is the result of using residual migration.

The area signified with 'A' shows the problems with using all of the data (top panel). Note how the gathers have tremendous, inconsistent curvature. When we discount this information (center panel) we get more reasonable gathers. Using residual migration to estimate $\Delta\mathbf{t}$ we can get the same, or better, gathers without throwing away a portion of the data. The problem with throwing away a portion of the data can been at 'C' and especially 'B'. We threw away the information that would help us flatten the reflector in order to avoid the problems seen in the top panel. Smply using vertical moveout analysis, it takes several non-linear iterations to achieve the same level of flatness at 'A' and 'B' that is seen with the first non-linear iteration using a residual migration measure.

Figure 8 shows every 15th CRP gather after five non-linear iterations. Note how the moveout in reflector at 'A' is virtually flat. Within valley structure, 'B', there is little remaining residual moveout. The most interesting location is 'C' where we are begining to see coherent events under the salt. Figure 9 shows the resulting velocity and image after five non-linear iterations. The salt top reflection is now clean. Note how the valley structure at 'A' is well imaged. At 'B' we can follow reflectors all the way to what appears to be the salt edge. On the top-left portion of the salt, 'C', we have gone from a jumbled mess (Figure 6) to being able to clearly follow reflectors. At 'D' we see a consitant, strong amplitude, salt bottom reflection. Finally, at 'E' we are begining to see strong events under the salt. Further improvement requires going to 3-D.

Another way to evaluate image improvement is to look at the γ values after successive iterations. Figure 10 show the γ values after zero to four iterations (left to right, top to bottom). The figure demonstrates that as we progress in iteration the γ value tends towards 1, indicating that the problem is converging.

CONCLUSIONS

Vertical moveout is inadequate method to characterize migration errors caused by velocity. By using residual Stolt migration more reasonable errors can be estimated and back projected. Early results indicate that the inverted result is more promising than simply using vertical positioning errors.

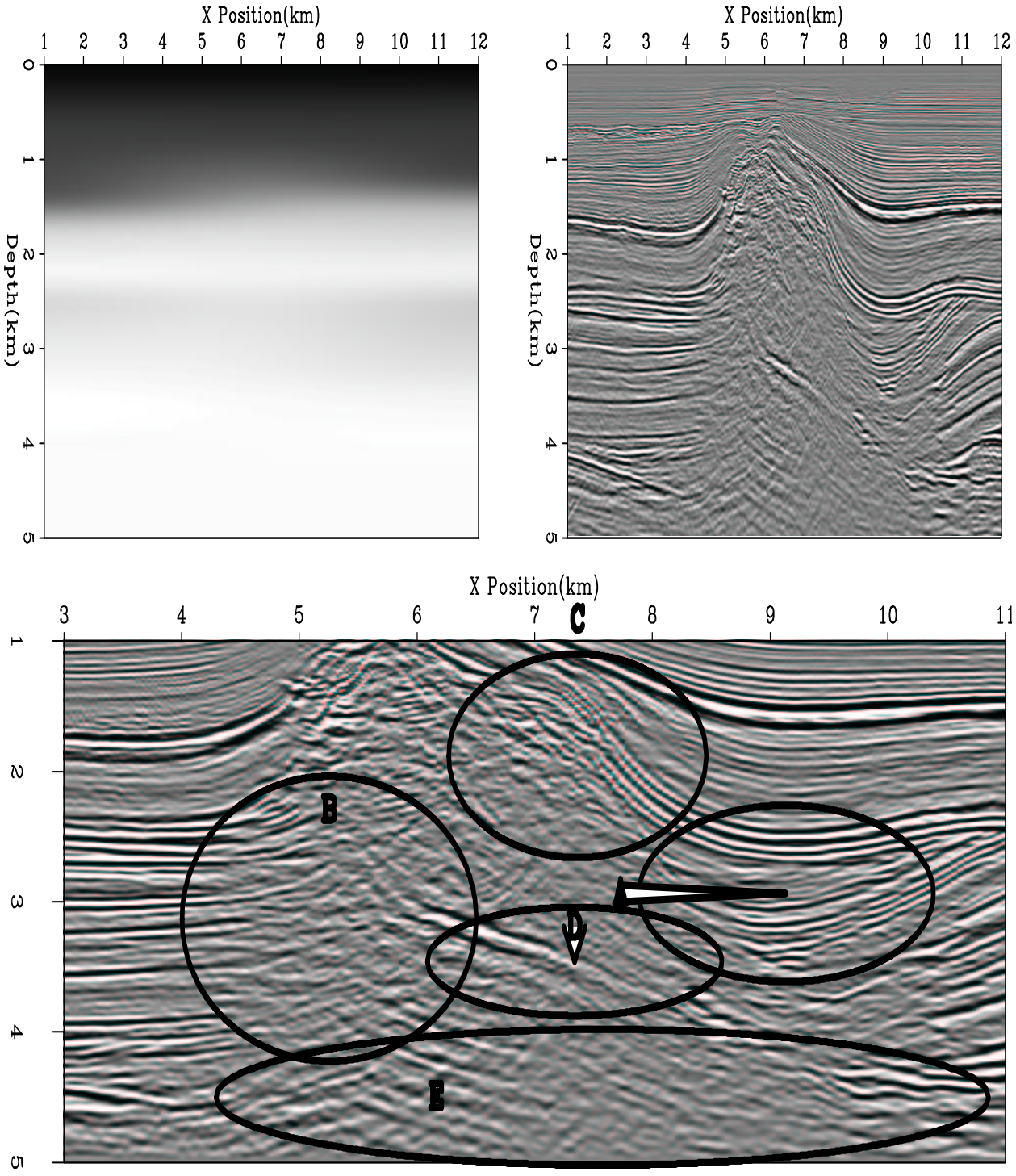

Figure 6: The initial model and migration. The top-left panel shows the velocity model and the top-right panel shows the migrated image using this velocity. The bottom panel shows a blow up around the salt body. 'A' - 'E' will be used later in the text for comparison. bob1-combo.vel0 [CR,M]

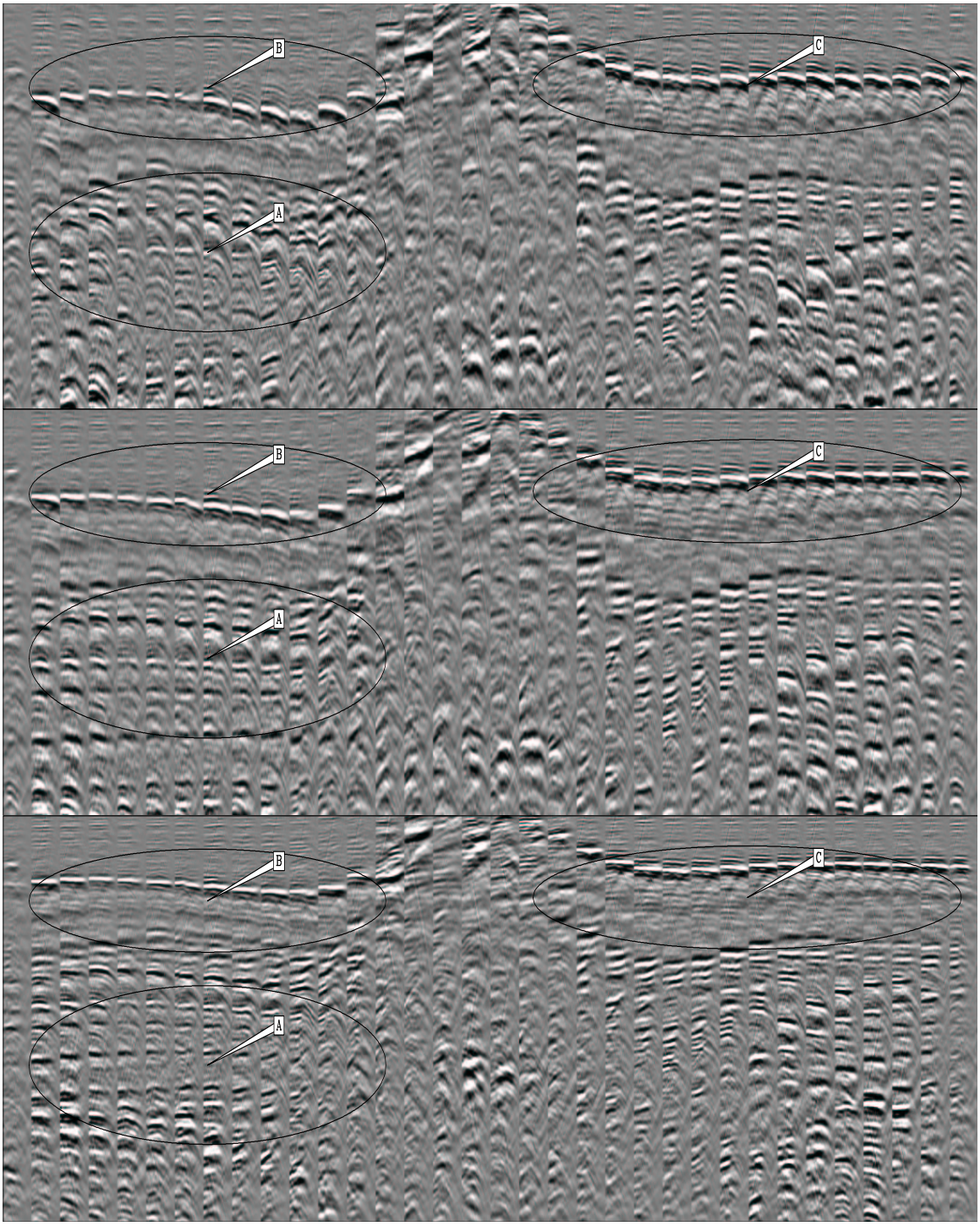

Figure 7: Each panel represents every 15th CRP gather between 1 and 4 km after one nonlinear iteration of tomography. The top panel is the result of performing tomography calculating $\Delta\mathbf{t}$ using vertical moveout. The center panel is using vertical moveout discounting data with significant moveout. The bottom panel shows the result of using residual migration as the basis of the $\Delta\mathbf{t}$ calculation. Note the improved flatness of the CRP gathers from top to bottom. bob1-gathers.iter1 [CR,M]

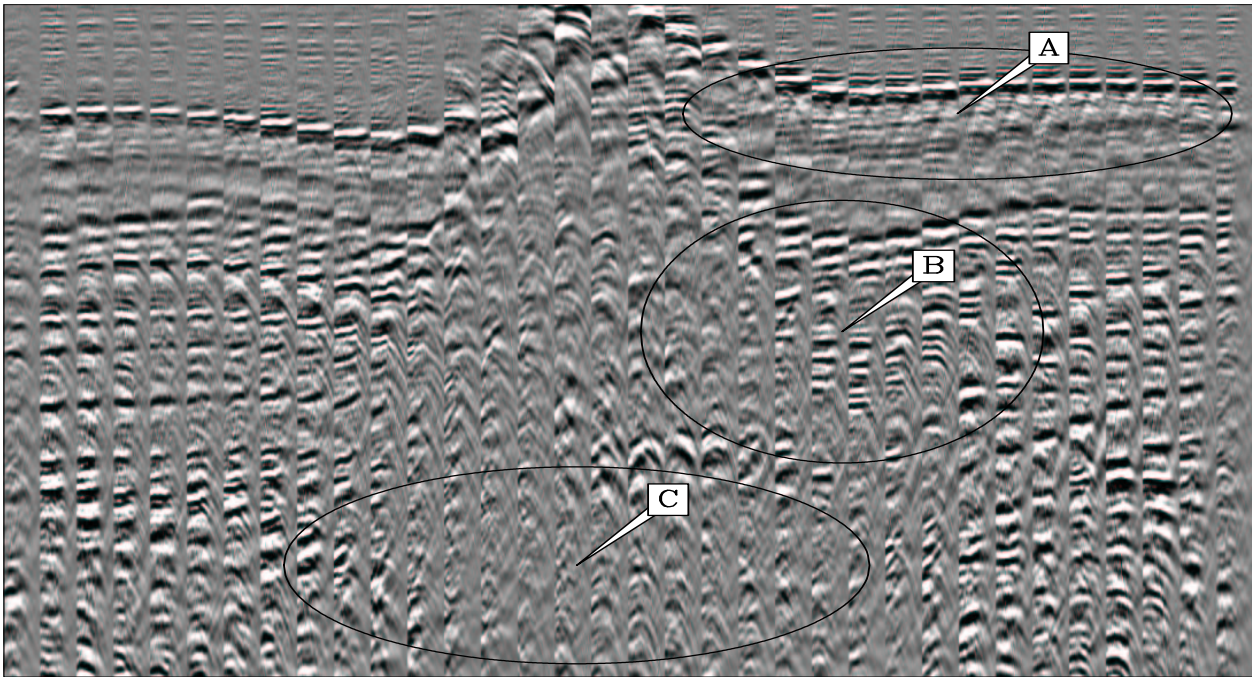

Figure 8: Every 15th CRP gather after five non-linear iterations. Note the flat gathers at ‘A’ and ‘B’ and the forming of coherent moveout below the salt at ‘C’. bob1-gathers.final [CR]

REFERENCES

Audebert, F., Diet, J. P., and Zhang, X., 1996, CRP-scans from 3-D pre-stack depth migration: A powerful combination of CRP-gathers and velocity scans:, *in* 66th Ann. Internat. Mtg Soc. of Expl. Geophys., 515–518.

Audebert, F., Diet, J. P., Guillaume, P., Jones, I. F., and Zhang, X., 1997, CRP-scans: 3-D preSDM velocity analysis via zero-offset tomographic inversion:, *in* 67th Ann. Internat. Mtg Soc. of Expl. Geophys., 1805–1808.

Biondi, B. L., and Palacharla, G., 1995, 3-D prestack depth migration of common-azimuth data:, *in* 65th Ann. Internat. Mtg Soc. of Expl. Geophys., 1197–1200.

Biondi, B., and Symes, W. W., 2002, Transformation to dip-dependent common image gathers: SEP–**112**, 65–82.

Clapp, R. G., and Biondi, B., 1999, Preconditioning tau tomography with geologic constraints: SEP–**100**, 35–50.

Clapp, R. G., and Biondi, B. L., 2000, Tau tomography with steering filters: 2-D field data example: SEP–**103**, 1–19.

Clapp, R. G., Fomel, S., and Claerbout, J., 1997, Solution steering with space-variant filters: SEP–**95**, 27–42.

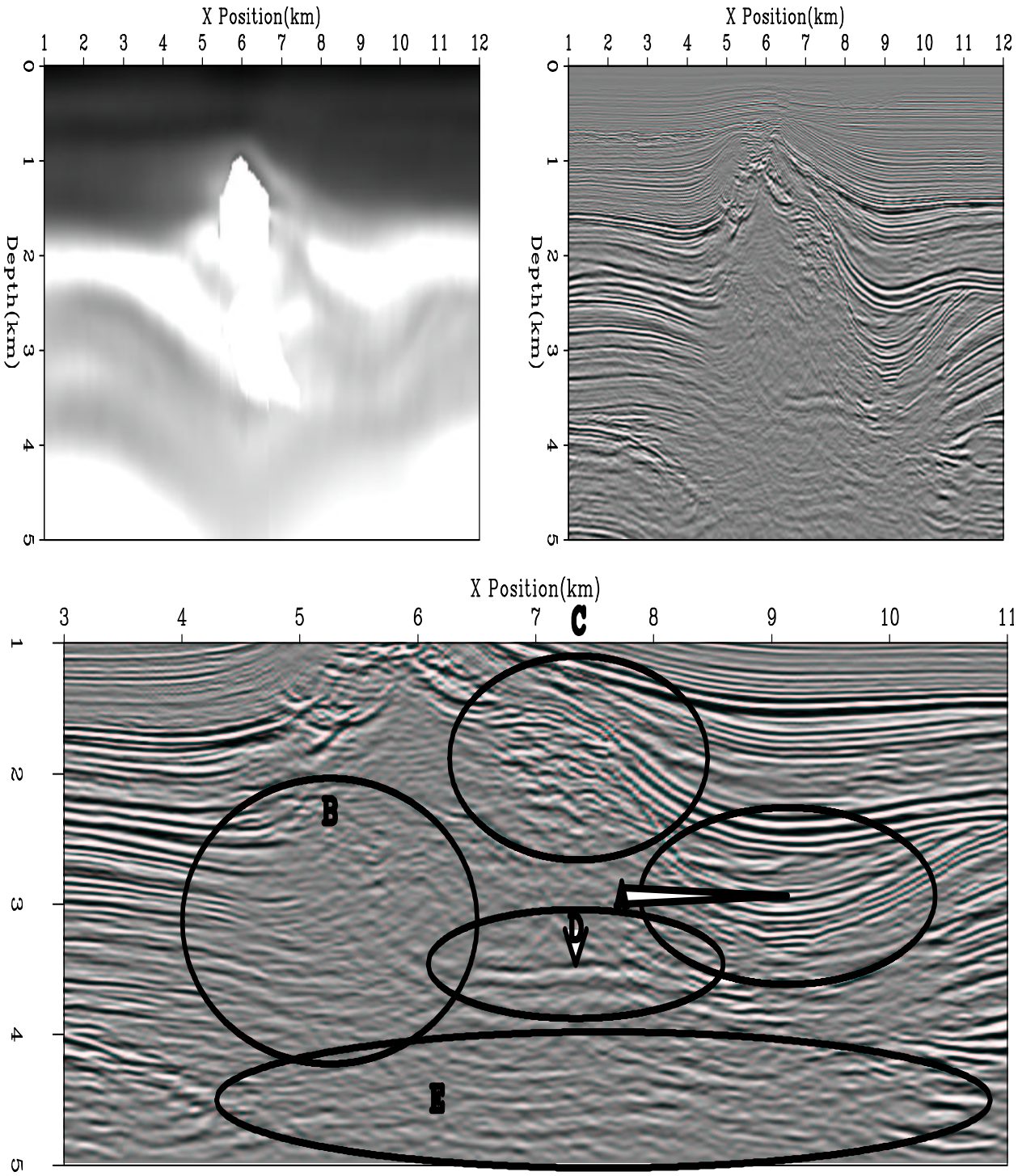

Figure 9: Data after five non-linear iterations of tomography with residual migration based moveout analysis. The top-left panel shows the velocity model and the top-right panel shows the migrated image using this velocity. The bottom panel shows a blow up around the salt body. Note how the valley structure at 'A' is well imaged. At 'B' we can follow reflectors all the way to what appears to be the salt edge. On the top-left portion of the salt, 'C', we have gone from a jumbled mesh (Figure 6) to being able to clearly follow reflectors. At 'D' we see a consistent, strong amplitude, salt bottom reflection. Finally, at 'E' we are begining to see the forming of fairly strong events under the salt. bob1-combo.final [CR,M]

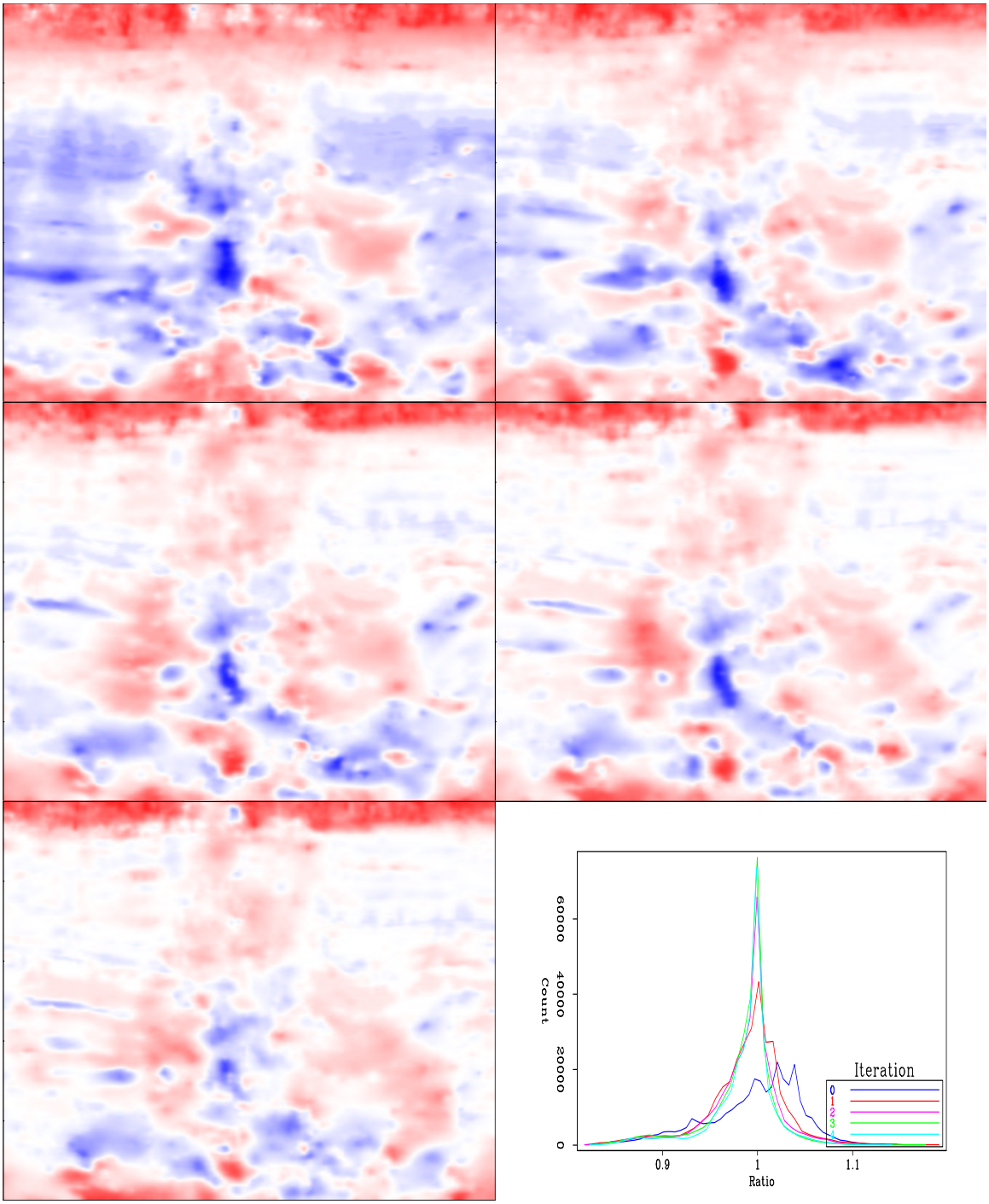

Figure 10: The residual moveout measure as a function of non-linear iteration. The top-left is the initial moveout, the top-right after one iteration, etc. The bottom-right panel shows a histogram for each of the γ maps. Note how the points cluster towards 1 as we progress in iteration. Note how the ratio tends towards 1 (no-moveout, white) as we progress. The red stripe on top is due to the severe early mute. The offset to angle transform has an edge effect that causes the data to curve up. As a result the best flatness is obtained with a very low γ value. These values are ignored in the inversion. bob1-ratios [CR,M]

Clapp, R. G., 2001, Geologically constrained migration velocity analysis: Ph.D. thesis, Stanford University.

Clapp, R. G., 2002, Dealing with errors in automatic velocity analysis: SEP–**112**, 37–46.

Etgen, J., 1990, Residual prestack migration and interval velocity estimation: Ph.D. thesis, Stanford University.

Fomel, S., Clapp, R., and Claerbout, J., 1997, Missing data interpolation by recursive filter preconditioning: SEP–**95**, 15–25.

Fomel, S., 1997, Velocity continuation and the anatomy of prestack residual migration:, *in* 67th Ann. Internat. Mtg Soc. of Expl. Geophys., 1762–1765.

Gazdag, J., and Sguazzero, P., 1984, Migration of seismic data by phase-shift plus interpolation: Migration of seismic data by phase-shift plus interpolation:, Soc. of Expl. Geophys., Geophysics, 124–131.

Levin, S. A., Rothman, D., and Rocca, F., 1983, Residual migration: Applications and limitations:, *in* 53rd Ann. Internat. Mtg Soc. of Expl. Geophys., Session:S10.7.

Prucha, M. L., Biondi, B. L., and Symes, W. W., 1999, Angle-domain common image gathers by wave-equation migration: SEP–**100**, 101–112.

Rocca, F., and Salvador, L., 1982, Residual migration:, *in* 52nd Ann. Internat. Mtg Soc. of Expl. Geophys., Session:S1.4.

Sava, P., and Fomel, S., 2000, Angle-gathers by Fourier Transform: SEP–**103**, 119–130.

Sava, P., 1999a, Short note–on Stolt common-azimuth residual migration: SEP–**102**, 61–66.

Sava, P., 1999b, Short note–on Stolt prestack residual migration: SEP–**100**, 151–158.

Stolt, R. H., 1996, Short note - a prestack residual time migration operator: Short note - a prestack residual time migration operator:, Soc. of Expl. Geophys., Geophysics, 605–607.

Stork, C., 1992, Reflection tomography in the postmigrated domain: Geophysics, **57**, no. 5, 680–692.